

NATURAL VENTILATION ASSESMENT OF AN EXISTING APARTMENT BUILDING IN THE MEDITERRANEAN USING TIME-DEPENDENT CFD

Eftychia Spentzou*¹, Malcolm Cook¹, Chih Lung Lin²

¹School of Civil and Building Engineering, Loughborough University, Leicestershire

LE11 3TU, UK

²Formerly School of Civil and Building Engineering, Loughborough University

*E.Spentzou@lboro.ac.uk

ABSTRACT

The benefits and limitations of time-dependent and steady state computational fluid dynamics simulations when evaluating natural ventilation were explored in a naturally ventilated case study apartment in the Mediterranean. For wind driven flows, indoor air properties responded quickly (i.e. within 1-min) to changing outdoor conditions, except indoor air temperatures (up to 30-min). The outdoor air temperature variations could reverse the flow direction during buoyancy-driven ventilation. Strong correlations between the steady state and transient simulation results were predicted (<1% error). Comparable indoor temperatures were found from simulations with both coarse and fine time steps, and up to 2% difference was found for indoor velocities.

INTRODUCTION

The potential of natural ventilation in achieving low-energy building design has been recognised over recent decades. Ventilation is important for occupants' indoor air quality (i.e. removal of stale air, odours and harmful chemicals), for removal of excess heat (i.e. natural cooling) and protection from condensation of the building fabric (CIBSE 2005). The benefits of natural ventilation are indisputable given the potential to reduce mechanical cooling load, improve indoor air quality, provide occupants' thermal comfort and deliver significant air change rates utilising wind, buoyancy induced airflows or a combination of both.

Air-tight buildings and recent ventilation rate reductions have contributed to reported concerns over indoor air quality (IAQ) (Lai et al., 2009). In hot climates, energy consumption for cooling has been predicted more than twice the energy for heating (Santamouris & Asimakopoulos, 1996). The reported heat waves contribute to further increase of the mechanical cooling peak load demand, disrupting supply (Kolokotroni et al., 2007). Further, a continuous rise of air-conditioning installations has been reported (Yun & Steemers, 2011), particularly in southern Europe (Geros et al., 1999).

Natural ventilation employs two distinct mechanisms; the natural forces of pressure difference induced by wind and the temperature gradients between internal and external thermal environments

(Jiru & Bitsuamlak, 2010). Measurements in urban canyons in Athens during the summer period have shown that the potential of natural single or cross ventilation is limited; reductions of up to 68% and 82% respectively, relative to undisturbed sites, have been reported (Georgakis & Santamouris, 2006). Enhancing the potential for buoyancy-driven ventilation in buildings in hot climates is important during windless days in order to meet comfort expectations (Linden, 1999).

Computational fluid dynamics (CFD) is widely used for the evaluation of natural ventilation because it offers high levels of detail and accuracy (Cook et al., 2003). CFD can be less expensive, both in time and resources, relative to traditional wind tunnel testing (Douglas et al., 2005). CFD also provides design flexibility, whole field data collection, and ease of evaluating different concepts and designs in controlled environments (Stavarakakis et al., 2010). The efficiency of the tool in evaluating natural ventilation has been proven by many, predicting good correlation with experimental and wind tunnel tests (Montazeri et al., 2010; Dehghan et al., 2013). Also, it has been shown effective to model dynamic thermal effects in buildings (Cook et al., 2008). Good correlation with semi-analytical results was predicted for the CFD software PHOENICS for both buoyancy and wind-driven ventilation flows (Papakonstantinou et al., 2000; Allocca et al., 2003).

The most common numerical approach in evaluating natural ventilation remains the steady state CFD, regardless of the latest development in turbulence modelling, improvement of technology and computer performance (Durrani, 2013). Ji et al. (2007) evaluated the performance of steady state CFD in modelling natural displacement ventilation flows driven by buoyancy forces in a single-storey space connected to an atrium, using the RNG $k-\epsilon$ turbulence model. When evaluating natural ventilation, it is important to consider the behaviour of the natural wind, varying in both speed and direction; a transient prediction would be appropriate in describing the flow (Jiang & Chen, 2002). Yuan and Glicksman (2008) explain that multiple steady states occur in combined buoyancy and wind-driven flows. Flynn and Caulfield (2009) investigated the hysteresis phenomenon due to ventilation forced by both internal heat sources and wind.

The study reported in this paper sought to evaluate the influence of varying environmental conditions on the natural ventilation performance of an apartment in the Mediterranean region using CFD simulations. The response time and the internal flow performance (e.g. hysteresis phenomenon) were predicted. The aim was to compare the benefits and limitations of time-dependent and conventional steady state computational modelling techniques and identify possible concerns when modelling natural ventilation.

Although others have undertaken similar research previously, this research is part of a project investigating the potential of energy refurbishments in Greece, using a case study building that is representative of over 4 million buildings in the country.

METHODOLOGY

For the purpose of this study, a case study apartment unit was selected, which is part of an existing 5-storey building in Athens and was constructed in the early 1970s. It consists of 4 living spaces: 2 with external-façade openings, 1 without external openings and 1 connected to an airshaft. Cross ventilation is achieved via the two façade openings and the airshaft at the rear (Figure 1). An extended description of the case study building and apartment designs are provided in (Spentzou et al., 2013).

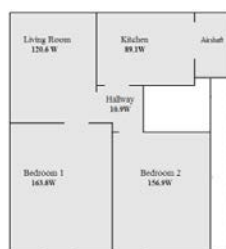


Figure 1 Layout of the apartment studied

For the CFD simulations the commercial well-established and validated CFD software package PHOENICS (CHAM Ltd., 2013) was used to solve the three-dimensional Reynolds Averaged Navier-Stokes equations using a steady state three dimensional structured Cartesian mesh. The external and internal openings remained fully open at all times. Sensible heat gains were modelled in the centre of each space.

The energy equation was solved for temperature, and buoyancy was modelled using the Boussinesq approximation. Turbulence was modelled using the Chen-Kim modified $k-\epsilon$ turbulence model for the study of the buoyancy driven flows (Chen & Kim, 1987) and for the wind-driven flows the model based on the Renormalization Group (RNG) methods (Yakhot & Orszag, 1986). The velocity components normal to each external opening were 'deduced'¹

¹ The in-flow values are deduced from the mass flow rate divided by the density and cell area (Ludwig & Mortimore, 2011).

with air pressure at the opening equal to the ambient and loss coefficient equal to $2.69 (=1/C_d^2)^{1/2}$.

Climate data representative of a day during the cooling period were selected. Boundary conditions included: varying values of dry-bulb temperature (between 19.3-29°C); specific humidity (0.88-1.12%); internal wall surface temperatures (20-28.8°C); and air mass flow through the openings (1.4-4.9 kg/m²/s). The hourly values were interpolated to finer time steps using INFORM² commands.

PHOENICS considers the ambient temperature as a fixed reference in the boundaries. In order to set time-dependent outdoor temperatures, profiles of outdoor air temperature could be assigned to the openings. However, this would result in additional buoyancy forces generated at the opening (i.e. fixed-variant temperatures). A decision was therefore made to modify the wall temperature (using a pseudo wall temperature) with respect to the external air temperature variations, and as follows:

$$T_{ps,wall} = T_w + (T_r - T_{out}) \quad (1)$$

where, $T_{ps,wall}$ is the pseudo wall temperature (°C), T_w the existing wall temperature, T_r the reference temperature and T_{out} the outdoor air temperature.

Table 1
Conditions of grid sensitivity test

M	IX	IY	IZ	Number of cells	CPU Time of run
A	30	33	46	45,540	3,338
B	36	38	46	62,928	4,627
C	38	38	56	80,864	5,851
D	52	54	67	188,136	14,753

In order to be certain that the solution was independent of the mesh resolution; four meshes were investigated (Table 1). The first two meshes provided similar results of velocity distribution along a measuring line at the apartment under study (Figure 2). Mesh B was selected in order to achieve balance between computational time and resolution.

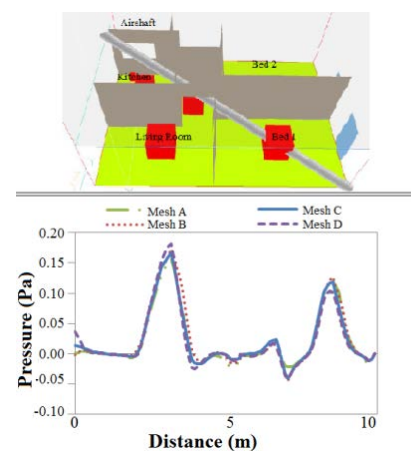


Figure 2 Measuring line and predicted air pressures for 4 different meshes

² Supplement to the PHOENICS input language facilitating the input of problem-defining data.

The resolution of time step should be selected according to the rate and scale of the environmental properties fluctuations. Smaller time steps are used for the simulation of quicker environmental changes, in order to detect the development of the state of the flow at each time step. However, an unnecessarily small time step would increase the computational time and load. For the purpose of this research, the time step was determined using two criteria: the change of input conditions between each time step; and the computational time required. In addition, a study was performed following the completion of the CFD simulations to assess the selection of time step with regard to both the response time of the output variables and the point in time after which negligible change of the solution occurs. A series of tests were conducted to identify the relationship between the change of each input variable and their converging iteration number. Time steps of one, five and 25 minutes were evaluated. The five-minute time step fitted the first two selection criteria as the change of input conditions was insignificant between each time step, the converging iteration number was similar for the smaller one minute step.

SIMULATIONS

Steps 1 to 4 below, detail the simulations that were performed. Table 2 presents the boundary conditions of each step and the variables selected.

Step-1: Steady state simulations were performed to evaluate the influence of the boundary and environmental condition (i.e. external air temperature, heat gains, indoor wall surface temperature, relative humidity and wind speed) variations as a one-step-change function on the: indoor air temperature; velocity; pressure; and relative humidity.

Step-2: A number of transient CFD simulations were performed with the environmental conditions

changing, to study the response time of buoyancy and/or wind-driven airflow regimes that steady state CFD simulations could not appropriately predict. The influence of outdoor air temperature increase (increments of 30-31°C and 30-32°C) and reductions to the wind speed (decrements of 3.8-3.3m/s and 3.8-2.8m/s) were investigated. All CFD models start from steady state and then the environmental factor changes as a one-step function. Each time step is one minute. The response time required to achieve steady state was evaluated.

Step-3: The airflow behaviour within the modelled spaces and adjacent airshaft was evaluated with respect to the difference between the internal and external thermal environments. Simulations were performed during buoyancy driven ventilation and with varying outdoor air temperatures (either increasing or decreasing). The influence of thermal mass on the direction of the flow was observed.

Step-4: A final time step sensitivity analysis was performed with regard to the criteria previously described (see Methodology) for five and 30 minutes time-steps to evaluate the accuracy of the time step used at the time-dependent simulations performed, for buoyancy and wind driven flows. The total period evaluated was 24-hours for wind driven flows and 1-hour for the computationally demanding buoyancy driven flows.

RESULTS AND ANALYSIS

Step-1: Influence of the environmental variables (Steady State)

The steady state simulations performed to investigate the effect of the variation of different parameters as a one-step-change function on the indoor air properties, predicted a linear relationship between the indoor and outdoor air temperatures. Indoor air velocity and pressure were dependent on the outdoor air temperature variations.

Table 2
Conditions of the CFD models for each of the four Steps performed

STEP	Simulations performed and Parameters Varied	Turbulence models used	DBT (°C)	Wall Temp(°C)	Sensible gain (W)	Specific humidity (%)	Mass flow (kg/m ² /s) or wind (m/s) @ openings	Time range_Time step
Step-1	1. 1: Change of Ambient Temperature (°C)	KECHEN	25-35	Adiabatic	Default	steady	Deduced: All	steady state
	1. 2: Change of Wall T (°C)		Fixed at 30	21-31	Adiabatic			
	1. 3: Change of Sensible (W)			Default		RH:18-78%		
	1. 4: Change of Humidity (%)	KERNG	Fixed at 30	Adiabatic	Default	steady	2.8-4.8 m/s at Beds' openings	
1. 5: Change of Wind (m/s)								
Step-2	2. 1: Change of DBT (°C)	KECHEN	30-31	Adiabatic	Default	steady	Deduced: All	1hour_1min
	2. 2: Change of Wind (m/s)	KERNG	30-32				2.8-2.4m/s	
	2. 3: Change of Wind (m/s)		Fixed at 30				2.8-2 m/s	
2. 4: Change of Wind (m/s)								
Step-3	3. Under only buoyancy driven	KECHEN	varying between 27.3 and 23.5	varying between 23.7 and 23.9	Varied gains only at the 2 bedrooms	varying between 0.98% and 0.91%	Deduced: All	5 hours_5 min
Step-4	4.1 Under wind driven	KERNG	19.3 to 29	23.7 to 26.4	fixed	0.88 to 1.12	1.42-4.87 kg/m ² /s	24 hours_5 & 30min
	4.2 Under only buoyancy driven	KECHEN	27.3 & 26	23.7	fixed	0.98 & 0.93	Deduced: All	1hour_5 & 30min

The increase of the sensible heat gain increased the indoor air temperature, almost linearly. It reduced the indoor air pressure in a non-uniform distribution across the spaces and dependent to the indoor-outdoor pressure difference, and increased the air velocity. The wall temperature, acting as an additional sensible heat gain, provided comparable relationships with the results of the sensible heat gain variations of the internal and external air properties. If the wall temperature rises, the internal air temperature and velocity would also increase.

Due to the use of the Boussinesq approximation, the air density would be fixed and unrelated to the humidity. Because the humidity would not influence the governing equations of the fluid, the air temperature, pressure and velocity would also not change with variations of the outdoor relative humidity. However, the relative humidity itself is a function of temperature, so the relative humidity in the building varies according to the value of temperature. On the other hand, the specific humidity was constant across the inner space and dependent on the specific humidity of the outdoor air (linear relation).

The effect of different wind speeds on the indoor environments was evaluated; the air speed was set normal to the openings varying between 2.8m/s and 4.8m/s. The increase of the wind speed resulted in a small indoor air temperature reduction and an increase of the indoor air velocity adjacent to the external openings (Figure 3). An indoor air pressure increase was predicted. The relationship between indoor air pressure and wind speed was quadratic.

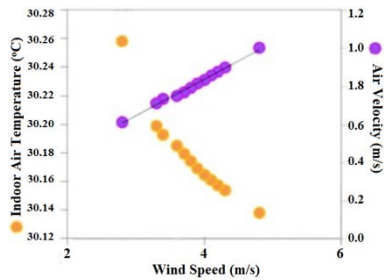


Figure 3 Indoor air velocity and temperature with regard to different wind speeds

Step-2: Response time of the flow regime

The relationship between the outdoor air temperature increase and the response of the indoor environment was evaluated. Simulations were performed for two levels of change (30-31°C and 30-32°C). It was predicted that approximately 10 to 15 minutes were required for the internal air temperature to become steady. A more rapid response was predicted for 1°C change of the DBT relative to the 2°C change, until 90% of the change was completed; deceleration occurred thereafter. Despite this, the total response time was comparable between the two levels of ambient change (30-31°C and 30-32°C). The increase

of outdoor temperature resulted in an initial decrease of the indoor air velocity (as the relative pressure was close to zero), followed by an increase after several minutes reaching the original levels within 15 to 20 minutes (Figure 4).

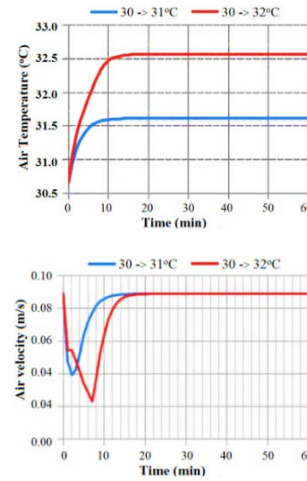


Figure 4 Response time of the indoor air temperature (top) and velocity (bottom) for two levels of DBT change (average value of the apartment studied at horizontal plane, 1m above the floor)

Table 3 summarises the response time of three indoor variables required to achieve 90% or 99% of change before they become steady, during varying outdoor air temperature or wind speed. The 99% response time of the air pressure and the air velocity was defined as the time required by these variables to reach 1% difference from the stable value. Higher response times were observed for larger ambient temperature changes. The response time required for the indoor air temperature to reach the 90% change was predicted to be approximately half of the 99% response time; for the air pressure and velocity, the 90% was approximately two thirds of the 99% response time. The initial rapid response of the indoor air variables to the outdoor temperature change considerably decreased after 90% of the change and until steady state was reached.

Table 3

Percentile of the response time of three indoor properties with regard to the DBT and wind speed variations

Change	Temperature (°C)		Pressure (Pa)		Velocity (m/s)	
	90%	99%	90%	99%	90%	99%
30-31°C	6.3	13.7	9.6	15.2	8.8	13.4
30-32°C	8.4	14.7	12.5	17	12.8	16.9
3.8-3.3m/s	13.6	25	<1	<1	<1	<1
3.8-2.8m/s	17.2	31.5	<1	<1	<1	<1

The response time varied considerably across the internal flow field. It was influenced by the magnitude and location of the internal heat sources. Figure 5 (bottom) demonstrates the percentage of temperature change for up to 30 minutes later, predicted along two measuring lines. Two tendencies

were observed: the response time increased close to the heat sources with regard to the amount of heat, and further increased with the increase of the room depth and distance from the openings.

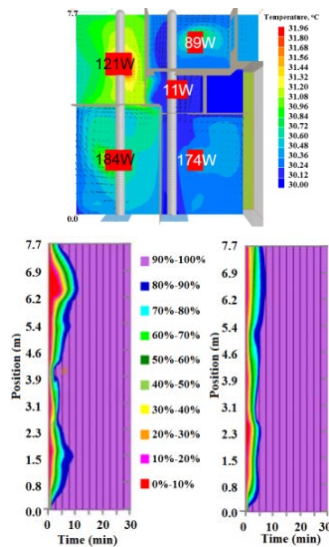


Figure 5 Plan view of the apartment studied (top) and the time dependent response of the indoor air temperature (bottom) at two measuring lines (top)

The relationship between the wind speed variations and the internal environment’s response was evaluated for two levels of change (3.8-3.3m/s and 3.8-2.8m/s). For a wind speed decrement of 0.5m/s the indoor air temperature would require up to 25 minutes to reach the 99% of change and finally steady state (Figure 4). This value increased further to 30 minutes, for a decrement of wind speed of 1m/s (Figure 6). The indoor air velocity responded instantly to the wind speed decrement (reaching 99% in less than two minutes), although reaching steady state within 15 to 20 minutes. A comparable response was predicted for the indoor air pressure, reaching steady state in one minute and experiencing small fluctuations for approximately 10 minutes.

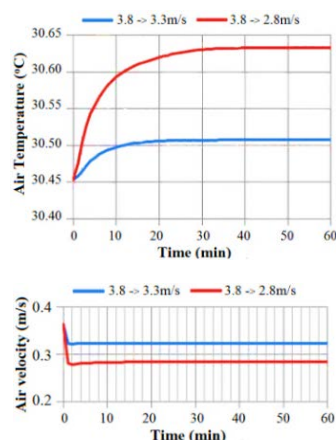


Figure 6 Response time of the indoor air temperature and velocity for two levels of wind speed change

The time-dependent simulations performed for two levels of change of outdoor air temperature (3 DBTs) and wind speed (3 wind speeds), predicted values of indoor air properties in agreement to the values predicted during the steady state simulations. Table 4 presents the average values (at 1m above the floor level) of stable indoor air temperature, pressure, and velocity using the two modelling techniques. The value of the time-dependent CFD is the predicted value of each variable after the outdoor temperature has changed for 60 minutes. The error between the two modelling techniques was less than 0.1% and 1%, for the varying outdoor air temperature and wind speed respectively. Time-dependent CFD could predict comparable results to those of steady state.

Table 4

Simulation results predicted with steady state and time dependent CFD simulations, for different values of wind speed and outdoor air temperature

	Temperature (°C)		Pressure (Pa)		Velocity (m/s)	
DBT, °C	31	32	31	32	31	32
Steady	31.62	32.57	-0.068	-0.067	0.0889	0.0889
Transient	31.62	32.57	-0.068	-0.067	0.0890	0.0890
Wind, m/s	3.3	2.8	3.3	2.8	3.3	2.8
Steady	30.51	30.64	0.3984	0.2837	0.3247	0.2823
Transient	30.51	30.63	0.396	0.2828	0.3239	0.2846

Step-3: Hysteresis phenomenon-Buoyancy

Simulations performed during buoyancy driven ventilation and for varying outdoor air temperatures, evaluated the airflow behaviour within the modelled spaces and adjacent airshaft.

Results predicted down flow (air flowing from the stack to the façade openings) during higher values of DBTs that exceeded the internal air temperature. Following the reduction of the DBT, the air speed decreased for a duration of about 2 hours (at 21:15) during which time, reverse flow occurred (Figure 7). The outdoor temperature had dropped below the indoor before the occurrence of reverse flow. The response time required by the flow regime could have resulted in the delay of reverse flow. The increase of the indoor air temperature before the occurrence of the reverse flow was small due to the corresponding reduction in the outdoor air temperature.

The relationship between the outdoor air temperature increase and the indoor air properties was also evaluated (Figure 8). Reverse flow from upwards to downwards occurred, when the outdoor air temperature slowly exceeded the internal. However, unlike the previously described strategy, the internal air temperature continuously increased together with the increase of the external temperature, and up until the reverse flow occurred. The internal air temperature was warmer than the external air due to the internal gains and the fully open openings. The up-flow continues until equilibrium is achieved between indoor and outdoor environments.

Following the down-flow, a significant increase of the indoor air velocity was observed, delivering temperature reduction in the spaces.

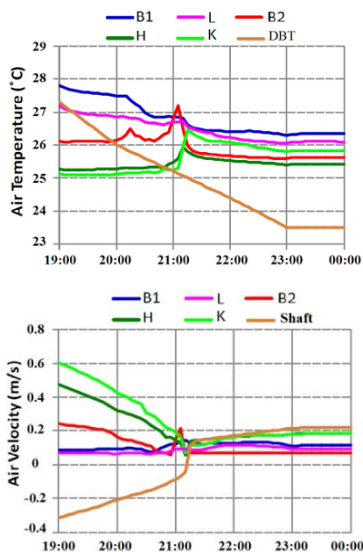


Figure 7 Predicted indoor air temperature (top) and velocity (bottom) at monitoring points at the centre of each space and the airshaft (1m height above the floor) during reducing outdoor temperatures

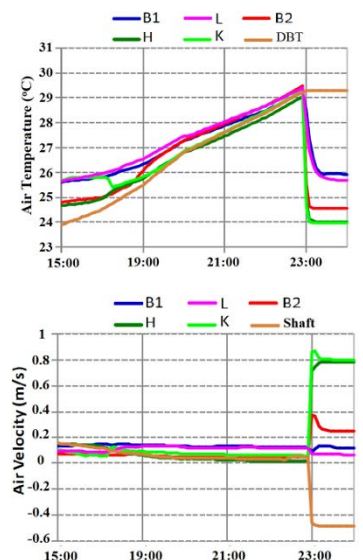


Figure 8 As for Figure 7, but during increase of the outdoor air temperature

Step-4: Time step Sensitivity Test

The size of the time step is highly significant during transient CFD simulations for the accuracy of the results. Different values of indoor air velocity and pressure were predicted for the buoyancy driven ventilation; the 30 minute time step predicted a smoother response curve relative to the five minute results. The simulations with larger time steps were predicted to be less sensitive to fluctuations of the outdoor environment (Figure 9). Despite this, comparable values of indoor air temperature were predicted for the five and 30 minute times steps

under both buoyancy and wind-driven ventilation (Table 5). Over a 24-hour period and during wind flows, similar results were predicted for the indoor air temperature and pressure during the two time steps, while the air velocities vary for no more than 2% (Figure 10). These errors would increase with increase of the environmental fluctuations; for this study the maximum changing rate of outdoor air temperature was 1.8°C per hour (-1.3°C per hour at 19:00).

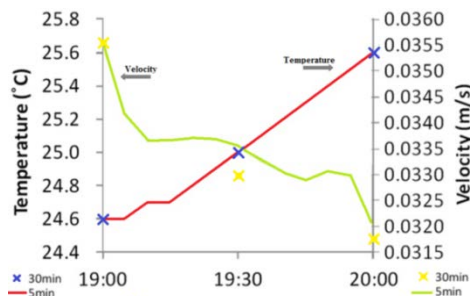


Figure 9 Response time of the indoor air velocity and temperature during buoyancy driven flow

Table 5

Maximum difference predicted between the simulation results of 30 and five minute time step

$$[(R_{30}-R_5)/R_5]$$

	Temperature	Pressure	Velocity
Buoyancy	0.00%	1.65%	1.71%
Wind	0.00%	0.07%	2.25%

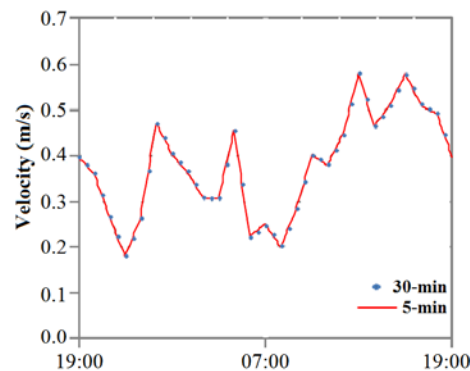


Figure 10 Response time of the indoor air velocity for two levels of wind speed change

DISCUSSION OF RESULTS

Simulation results predicted that the response time of the indoor air characteristics is dependent on three factors: (a) the type of boundary condition changing; (b) the amount of boundary condition change; and (c) the distribution of the energy, momentum, or mass sources and space geometry (e.g. depth). The response time of the flow regime varied with regard to the types of boundary condition, the energy sources (e.g. heat gains and ambient temperature) and the momentum sources (e.g. wind). The response of the indoor air temperature (i.e. energy) was predicted to be more time demanding (tens of minutes)

regardless of the type of boundary condition varying. However, a more rapid airflow rate response was expected for variations in the sources of momentum.

Larger changes of the boundary conditions resulted in longer indoor airflow response times. However, the increment of response time was not directly proportional to the change of boundary conditions: twice the increment of the temperature source required 13% more response time; four times more decrement of the pressure source (or double decrement of wind speed) required 25% more response time. Furthermore, the longer the distance from the changing environmental source, the more response time would be required for that variation. On the contrary, zones adjacent to heat sources require greater response time to reach stable temperatures. A larger number of sources within the spaces could potentially buffer the change of state and magnify the response time.

The fluctuations of wind speed resulted in up to 30 minutes response time for the indoor air temperature. This value was significantly higher than the response time with respect to DBT variations, and could further increase for larger wind speed fluctuations. Air velocity and pressure responded faster to the variation of the wind speed (e.g. less than two minutes), rather than for variations of the DBT (9-17 minutes until 99% change). These findings could be valuable during the preliminary design stage of natural ventilation strategies in buildings, for either wind or buoyancy driven flows.

Steady state CFD simulations could be used to efficiently evaluate the change of the flow regime in response to the change of the outdoor air properties. If all the sources of air temperature or mass had the same amount of change and the momentum source was unvaried, the resulted temperature or mass change would be the same everywhere in the flow regime. Otherwise, the pattern of flow regime would vary. Time dependent CFD simulations could further calculate the time required for the transformation of the flow regime, as well as, the flow behaviour between the different states. This information is valuable for the evaluation of control strategy during the design stage for natural ventilation.

Results of the buoyancy-driven simulation indicate slow response of the internal flow. The response time was dependent on the building's thermal mass, and the number and size of openings. If the building was extremely lightweight, the response of airflow could become faster and the difference between the time-dependent and steady state results negligible. Therefore, the computational technique should be selected also with regard to the building characteristics and design. On the contrary, during wind driven ventilation, simulation results suggest immediate response of the indoor air velocity and pressure. Results from the time step sensitivity analysis were independent on the time step's size.

Therefore, it could be assumed that the response time of wind-driven airflow was so short that the flow regime became stable at each time step. The airflow responded quickly to the wind speed fluctuations due to the lack of other momentum sources in the building, which could buffer that change.

Time-dependent CFD simulations predicted the hysteresis effect (i.e. a different response time when the environmental change was in an opposite trend) of the airflow, which is highly important when designing buoyancy driven ventilation strategies. Reverse of flow upwards to downwards, when considered during the design stage could be utilised to deliver significant temperature reduction, as shown in Figure 8.

Lastly, one of the limitations of this work was the use of the pseudo-wall-temperature to assess the time-dependent behaviour of the airflow. This method could affect the accuracy of airflow pattern if the change of outdoor temperature was faster than the speed of indoor heat convection.

CONCLUSION

This paper reported the results of a numerical study focused on the differences between the time-dependent and steady state CFD simulations when modelling natural ventilation. The response time of the indoor air properties to the changing outdoor conditions was predicted as low as one minute for wind-driven flows, depending on: the type of boundary conditions varied; the fluctuation range; and the distribution of heat sources in the spaces. Indoor air temperature experiences the slowest response time, reaching up to 30 minutes, compared to the air velocity and pressure.

Strong correlation between the steady state and transient simulation results was observed with less than 0.1% error and 1%, for outdoor air temperature and wind speed variations, respectively. Further to this, transient simulations provided detailed information regarding the hysteresis effect of the flow, as well as the changing process of the airflow. The time step sensitivity study predicted that the use of coarser time step provided comparable simulation results of air temperature to the finer, although different for some values, by up to 2% for the air velocity.

This research will continue with the performance evaluation of applied natural ventilation strategies in a case study apartment building under various climatic scenarios, and the potential of these strategies in delivering occupants' thermal comfort expectations.

ACKNOWLEDGEMENT

We would like to acknowledge the technical support provided by CHAM.

REFERENCES

- Allocca, C., Chen, Q., Glicksman, L.R. 2003. Design analysis of single-sided natural ventilation, *Energy and Buildings*, 35(8), pp785-795.
- CHAM Ltd. 2013. PHOENICS software, version 2012 (64bit Intel), UK Headquarters Concentration, Heat and Momentum Limited, Wimbledon Village, London.
- Chen, Y.S., Kim, S.W. 1987. Computation of turbulent flows using an extended k-epsilon turbulence closure model, NASA-CR-179204, United States.
- CIBSE 2005. CIBSE Guide B. Heating, ventilating, air conditioning and refrigeration. London, UK.
- Cook, M.J., Ji, Y., Hunt, G. 2003. CFD modelling of natural ventilation: combined wind and buoyancy forces, *International Journal of Ventilation*, 1(3), pp169-180.
- Cook, M.J., Zitzmann, T., Pfrommer, P. 2008. Dynamic thermal building analysis with CFD – modelling radiation. *Journal of Building Performance Simulation*, 1(2), pp117-131.
- Dehghan, A.A., Esfeh, M.K., Manshadi, M.D. 2013. Natural ventilation characteristics of one sided wind catchers, experimental and analytical evaluation, *Energy and Buildings*, 61, pp366-377.
- Douglas, J.F., Gasiorek, J.M., Swaffield, J.A., Lynne, B.J. 2005. *Fluid Mechanics*. 5th, Essex, England, Pearson Education Limited.
- Durrani, F. 2013, Using Large Eddy Simulation to model buoyancy-driven natural ventilation, Loughborough University.
- Flynn, M.R., Caulfield, C.P. 2009. Effect of volumetric heat sources on hysteresis phenomena in natural and mixed-mode ventilation, *Building and Environment*, 44(1), pp216-226.
- Georgakis, C., Santamouris, M. 2006. Experimental investigation of air flow and temperature distribution in deep urban canyons for natural ventilation purposes, *Energy and Buildings*, 38(4), pp367-376.
- Geros, V., Santamouris, M., Tsangrasoulis, A., Guarracino, G. 1999. Experimental evaluation of night ventilation phenomena, *Energy and Buildings*, 29(2), pp141-154.
- Ji, Y., Cook, M.J., Hanby, V. 2007. CFD modelling of natural displacement ventilation in an enclosure connected to an atrium, *Building and Environment*, 42(3), pp1158-1172.
- Jiang, Y., Chen, Q. 2002. Effect of fluctuating wind direction on cross natural ventilation in buildings from large eddy simulation, *Building and Environment*, 37, pp379-386.
- Jiru, T.E., Bitsuamlak, G.T. 2010. Application of CFD in modelling wind-induced natural ventilation of buildings - A review, *International Journal of Ventilation*, 9(2), pp131-147.
- Kolokotroni, M., Zhang, Y., Watkins, R. 2007. The London heat island and building cooling design. *Solar Energy*, 81(1), pp102-110.
- Lai, A.C.K., Mui, K.W., Wong, L.T., Law, L.Y. 2009. An evaluation model for indoor environmental quality (IEQ) acceptance in residential buildings, *Energy and Buildings*, 41(9), pp930-936.
- Linden, P.F. 1999. The fluid mechanics of natural ventilation, *Annual review of Fluid Mechanics*, (31), pp201-238.
- Montazeri, H., Montazeri, F., Azizian, R., Mostafavi, S. 2010. Two-sided wind catcher performance evaluation using experimental, numerical and analytical modelling, *Renewable Energy*, 35(7), pp1424-1435.
- Papakonstantinou, K., Kiranoudis, C., Markatos, N. 2000. Numerical simulation of air flow field in single-sided ventilated buildings, *Energy and Buildings*, 33(1), pp41-48.
- Santamouris, M., Asimakopoulos, D. 1996. *Passive cooling of buildings*, London, UK, James & James Ltd.
- Spentzou, E., Cook, M., Emmitt, S. 2013. Enhancing Indoor Comfort in Existing Apartment Buildings in Athens Using Natural Ventilation. In: *13th Conference of International Building Performance Simulation Association*. Chambéry, France, IBPSA, August 26-28.
- Stavrakakis, G.M., Zervas, P.L., Sarimveis, H., Markatos, N.C. 2010. Development of a computational tool to quantify architectural-design effects on thermal comfort in naturally ventilated rural houses, *Building and Environment*, 45(1), pp65-80.
- Yakhot, V., Orszag, S.A. 1986. Renormalization group analysis of turbulence, I. Basic theory, *Journal of Scientific Computing*, 1(1), pp3-51.
- Yuan, J., Glicksman, L.R. 2008. Multiple steady states in combined buoyancy and wind driven natural ventilation: The conditions for multiple solutions and the critical point for initial conditions, *Building and Environment*, 43(1), pp62-69.
- Yun, G.Y., Steemers, K. 2011 Behavioural, physical and socio-economic factors in household cooling energy consumption, *Applied Energy*, 88(6), pp2191-2200.